Modeling the chemical structure of spray flames using tabulated chemistry method

B. Franzelli[a,b,*], B. Fiorina[a,b], N. Darabiha[a,b]
[a] Ecole Centrale Paris, Grande Voie des Vignes, 92290 Châtenay-Malabry, France
[b] CNRS, UPR 288, Laboratoire d'Energétique Moléculaire et Macroscopique, Combustion (EM2C), Grande Voie des Vignes, 92290 Châtenay-Malabry, France
benedetta.franzelli@ecp.fr and benoit.fiorina@ecp.fr and nasser.darabiha@ecp.fr

Abstract

Flamelet-based tabulated chemistry methods have initially been developed to introduce detailed chemistry in gaseous flames with a reasonable computational cost. Although being attractive, their performance to predict the complex structure of spray flames presenting both premixed-like and diffusion-like reactive layers has never been rigorously identified. A new technique called Partially-Premixed Flamelet tabulation (2PTF) is proposed in this paper to tackle the chemical structure of spray flames. In the 2PTF method, information from partially-premixed flames are stored into a 3-D look-up table parametrized as function of the progress variable Y_c, of the mixture fraction Y_z, and of the scalar dissipation χ^*. The 2PTF results are compared to different tabulated chemistry strategies are here considered: the PFT method, based on premixed flamelets, and the DFT approach, based on diffusion flame elements.

The three techniques have initially been tested on1-D laminar axisymmetric counterflow kerosene/air gaseous flames and then on laminar counterflow spray flames over a wide range of conditions (injection droplet size, velocity and equivalence ratio). For all considered situations, the result analysis shows that 2-D (Y_c,Y_z) chemical tables (PFT and DFT) are not able to model spray combustion. The new 3-D chemical look-up table constructed from 2PTF methodology accurately captures the flame structure for all studied cases. It clearly demonstrates that a gaseous flamelet library works in spray combustion on the condition that the chemical table has the adequate number of dimension.

1. Introduction

The complete comprehension of spray combustion, necessary to guarantee security and to reduce pollutant emissions in aircraft combustions and internal combustion engines, is an active research topic [1]. Spray combustion is generally characterized by liquid dispersion into droplets and evaporation, which causes strong inhomogeneities of equivalence ratio in the fresh gases and the flame front. As a consequence, the chemical structure of spray flames presents both premixed-like and diffusion-like reactive layers [2, 3] and the numerical prediction of phenomena sensitive to detailed chemistry, such as the pollutant predictions or the flame propagation, is very challenging.

Flamelet-based tabulated chemistry methods have initially been developed to introduce detailed chemistry in gaseous flames but, although being attractive, their performances have never been completely investigated for spray combustion. Tabulated chemistry methods assume that the turbulent flame structure is similar to those of flamelet elements based on a single burning regime. For instance, Premixed Flamelet Tabulation (PFT) methods are based on fully-premixed laminar flamelets [4, 5], whereas the Diffusion Flamelet Tabulation (DFT) techniques rely on laminar diffusion flamelets [6, 7]. Only recently, multi-regime flamelet methods have been proposed to model the structure of complex flames where both premixed-like and diffusion-like reactive layers are present [8, 9, 10, 11]. Hollmann and Gutheil [12] observed that a laminar gas library based on a single combustion regime cannot correctly reproduce the structure of a spray flame since premixed-like, partially premixed-like or diffusion-like features could be found depending on the boundary conditions. To capture these complex regimes, they proposed a tabulated chemistry method directly based on spray flamelets. This strategy is consistent but requires a very high dimensional library as all physical spray parameters have to be varied (droplet diameter, liquid volume fraction, liquid injection velocity,..). A more efficient solution would be to tabulate only the chemical subspace effectively accessed by spray combustion. A possible strategy would be therefore to identify this subspace from gaseous flame elements as in [4, 5, 10, 13]. This point has been already observed by Baba and Kurose [14] who mentioned the needing of a combustion model for partially premixed flames to guarantee the prediction accuracy of spray jet flames.

*Corresponding author: benedetta.franzelli@ecp.fr

The present article discusses the chemical structure modeling of spray flames using tabulated chemistry methods by assuming that the chemical subspace effectively covered by spray combustion can be covered by a collection of gaseous flamelets. Three tabulated chemistry strategies are introduced in Section 2. The PFT method, based on premixed flamelets, the DFT approach, based on diffusion flame elements, and a new technique called Partially-Premixed Tabulated Flamelet tabulation (2PTF). The 2PTF method, based on the tabulation of partially-premixed flamelets, is proposed to tackle complex chemical structure presenting both premixed-like and diffusion-like reactive layers. The performances of this tabulated chemistry strategy is initially tested on gaseous partially-premixed flames in Section 3 and compared to those of the classical PFT and DFT techniques. In Section 4 the investigated spray configuration, a 1-D axisymmetric conterflow spray flame, is described. All tabulation techniques are then tested in Section 5 on the spray configuration with an a priori analysis. As the structure of spray flames is highly sensitive to the boundary conditions, the performances of tabulated chemistry methods for spray combustion are finally assessed for different injection velocities, droplet diameters and overall equivalence ratio.

2. Chemistry tabulation from gaseous flamelets

Predicting the flame structure and the pollutant formation of spray combustion requires careful description and comprehension of the chemical phenomena. Tabulated chemistry is a popular technique to account for detailed chemical effects with a reasonable computational cost [15]. Among the different strategies to generate chemical look-up tables, some of them are based on physical considerations like the PFT or the DFT methods. These approaches assume that the composition space accessed by a turbulent flame is determined by a reduced set of variables such as the progress variable Y_c, evolving monotonically between fresh and burnt gases [16]:

$$Y_C = Y_{CO} + Y_{CO_2} \tag{1}$$

and the mixture fraction Y_z, representing the local mixture equivalence ratio:

$$Y_z = \sum_{k=1}^{N_{spec}} n_{Ck} \frac{Y_k W_C}{W_k}, \tag{2}$$

where W_C is the element weight of carbon, W_k and n_{Ck} are the molar weight and the number of carbon atoms for the k^{th} species, respectively.

2.1 The PFT methods

PFT methods, such as FPI (Flame prolongation of ILDM [4]) or FGM (Flamelet Generated Manifold [5]), assume that the chemical subspace accessed by a flame can be mapped by a collection of 1-D gaseous laminar premixed flames computed using detailed chemistry for various equivalence ratios $\phi_L < \phi < \phi_R$ within the flammability limits. Any thermo-chemical quantity φ is then stored in a 2-D look-up table:

$$\varphi = \varphi^{PFT}[Y_c, Y_z], \tag{3}$$

where φ^{PFT} is obtained from laminar premixed flamelets. The rich ϕ_R (lean ϕ_L) flammability limit is defined as the maximal (minimal) possible value of the equivalence ratio of a premixed flame. Above (below) that point, a freely-propagating premixed planar laminar flame will extinguish.

2.2 The DFT methods

In the DFT method, such as the flamelet model [6] or the FPV (Flamelet/Progress Variable) model [7]. any thermo-chemical quantity φ is obtained from a look-up table built from gaseous strained diffusion flames for different values of the strain rate $0 < a < a^{ext}$, where a^{ext} is the extinction limit:

$$\varphi = \varphi^{DFT}[Y_c, Y_z]. \tag{4}$$

Both PFT and DFT methods assume a single burning regime and that the chemical structure of flames evolves in a 2-D (Y_c,Y_z) subspace. However, as demonstrated in [10, 13], for partially-premixed flames the effective dimension of the composition space accessed by the chemical trajectories is higher. In such situations, supplementary coordinates such as the scalar dissipation rate for the mixture fraction and/or for the progress variable should be added.

An enhanced tabulated chemistry method called 2PTF is proposed in next section to increase the range of validity of the model. As suggested by [10], a coordinate related to the mixture fraction scalar dissipation rate is added to the chemical look-up table in order to tackle complex chemical structure presenting both premixed-like and diffusion-like reactive layers.

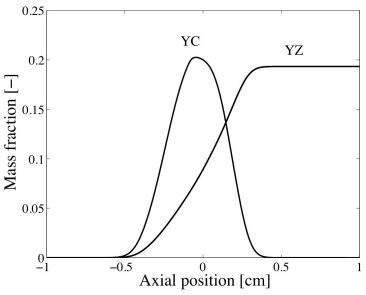

Figure 1. Mixture fraction Y_z and progress variable Y_c as a function of the axial position in the gaseous flame.

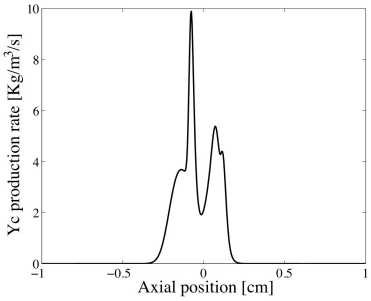

Figure 2. The production rate of the progress variable $\dot{\omega}_{Y_c}$ obtained with the detailed mechanism for the gaseous flame.

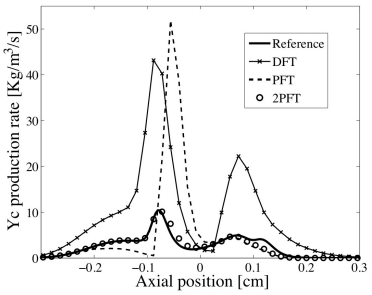

Figure 3. The production rate $\dot{\omega}_{Y_c}$ of the gaseous flame obtained with the detailed chemistry is compared to the a priori profiles for three tabulated mechanisms.

2.3 The Partially-Premixed Tabulated Flamelet method

In the 2PTF method, it is assumed that the chemical flame structure of a complex flame is mapped by a collection of 1-D gaseous partially-premixed counterflow flamelets characterized by an injection of pure air against a fuel/air mixture at equivalence ratio ϕ^f for a given value of strain rate a. The table is then built by varying the fuel/air stream equivalence ratio between $\phi^f = \phi^f_L$ and $\phi^f = +\infty$, where ϕ^f_L is the smallest value of the fuel/air stream equivalence ratio for which the counterflow flame is stabilized, and solving the flamelet for different values of the strain rate $0 < a < a^{ext}$.

The limit of the 2PTF table tends towards PFT and DFT tables respectively. Indeed when $\phi^f = +\infty$ and $0 < a < a^{ext}$ the table is filled by diffusion flamelets as in DFT. At the opposite when $a = 0$ and $\phi_L < \phi^f < \phi_R$ the table is filled with unstrained laminar premixed flames as in PFT. The 2PTF method is then based on different archetypal flamelets to map the subspace accessed by both premixed and non-premixed flames. This subspace is identified by three parameters: the progress variable Y_c, the mixture fraction Y_z and the scalar dissipation rate χ^* of Y_z:

$$\chi^* = \rho_0 D_0 |\nabla Y_z|^2, \tag{5}$$

where ρ_0 and D_0 are a reference density and diffusion coefficient, respectively. For each point (Y_c,Y_z,χ^*) covered by the database there is only one corresponding flamelet and any thermo-chemical quantity φ is then obtained from the 3-D look-up table:

$$\varphi = \varphi^{2PTF}[Y_c, Y_z, \chi^*]. \tag{6}$$

3. Modeling the chemical structure of gaseous partially premixed combustion

The performances of the three tabulation methods have been initially evaluated on gaseous partially-premixed kerosene/air flames. In the following, all spray and gaseous flames have been simulated with the REGATH-counterflow code [17, 18] using a detailed mechanism comprising $N_{spec} = 74$ species and $N_{reac} = 991$ reactions [19]. To simplify the calculation, kerosene is represented by the $C_{10}H_{22}$ species and unity Lewis number is assumed for all species.

The PFT table is built from a collection of adiabatic gaseous premixed flames for $\phi_L < \phi < \phi_R$ whereas the DFT table is based on adiabatic gaseous diffusion flames for different values of the injection velocity comprised between $0.2\ m/s$ and $10\ m/s$. The 2PTF table is composed by a collection of adiabatic gaseous counterflow flames for $1.6 < \phi^f < +\infty$ ($0.1 < Y^f_{C10H22} < 1.00$) and for different values of the injection velocity within the extinction limit. The injection temperature of fresh gases is equal to $T = 400\ K$ in all flamelets.

As example, the performances of the three tabulated methods are evaluated on a gaseous partially-premixed kerosene/air flame. Pure air is injected on the left side (identified by superscript ox) at $x = -1\ cm$ against a fuel/air stream $\phi^f = 4.45$ injected on the right side (superscript f) at $x = 1\ cm$. The injection velocity and temperature are the same for both sides, i.e. $v^f = v^{ox} = 0.2\ m/s$ and $T^f = T^{ox} = 400\ K$ respectively. The mixture fraction Y_z is maximum near the fuel/air mixture injection ($x > 0.5\ cm$) and decreases to zero near the pure air injection ($x < -0.5\ cm$), whereas the progress variable Y_C identifies the reaction zone (Fig. 1). The chemical source term, i.e. the production rate of the progress variable $\dot{\omega}_{Y_c}$ (in $kg/m^3/s$) obtained with the detailed mechanism presents two peaks (Fig. 2). A first reaction region is found for $0 < x < 0.2\ cm$, where the injected

mixture burns in a premixed-like regime, and a second reaction zone at $x \approx 0.1\ cm$ where products recombine with pure air coming from the left side.

3.1 A priori test

The behavior of the tabulated mechanisms is evaluated with an a priori analysis comparing the tabulated quantities to the reference solution obtained with the detailed scheme. For each point of the detailed mechanism solution, the values of progress variable Y_c, mixture fraction Y_z and χ^* are evaluated using Eqs. (1)-(2) and (5). The tabulated chemical source terms are then extracted from the PFT, DFT and 2PTF look-up tables: $\dot{\omega}_{Y_c}^{PFT}[Y_c, Y_z]$, $\dot{\omega}_{Y_c}^{DFT}[Y_c, Y_z]$ and $\dot{\omega}_{Y_c}^{2PTF}[Y_c, Y_z, \chi^*]$ respectively. The tabulated chemical source term are compared to the reference $\dot{\omega}_{Y_c}$ obtained with the detailed chemistry in Fig. 3 (PFT-dotted gray line, DFT-gray cross symbols, 2PTF-black dotted symbols). The PFT method correctly predicts $\dot{\omega}_{Y_c}$ in the first premixed-like reaction zone, whereas the DFT method globally overestimates it. Only the 2PTF method correctly reproduces the whole reaction zone by covering both premixed-like, partially-premixed-like and diffusion-like regimes.

3.2 A posteriori test

The performances of the tabulated mechanisms are now evaluated in a posteriori way. The counterflow gaseous flames are now solved using the classical tabulation technique [4, 5]. The species conservation equations:

$$\rho v \frac{\partial Y_k}{\partial x} = -\frac{\partial}{\partial x}\left(\rho Y_k V_{kx}\right) + W_k \dot{\Omega}_k \quad for \quad k = 1, .., N_{spec} \tag{7}$$

with ρ the mixture density, v the axial velocity, V_{kx} the diffusion velocity in the axial direction, $\dot{\Omega}_k = \dot{\omega}_k / W_k$ the molar chemical production rate, are replaced by a conservation equation for Y_z and Y_c:

$$\rho v \frac{\partial Y_z}{\partial x} = -\frac{\partial}{\partial x}\left(\rho Y_z V_{Y_z x}\right) \tag{8}$$

$$\rho v \frac{\partial Y_c}{\partial x} = -\frac{\partial}{\partial x}\left(\rho Y_c V_{Y_c x}\right) + W_{Y_c} \dot{\Omega}_{Y_c}, \tag{9}$$

where the chemical source term $\dot{\omega}_{Y_c} = W_{Y_c}\dot{\Omega}_{Y_c}$ is either closed from the PFT, DFT and 2PTF look-up table: $\dot{\omega_{Y_c}}^{PFT}$, $\dot{\omega_{Y_c}}^{DFT}$ and $\dot{\omega_{Y_c}}^{2PTF}$ respectively. The quantity χ^* is calculated from the solved Y_z profile.
The profiles obtained after the calculation (namely the a posteriori results) are compared to the solution of the detailed mechanism in Fig. 4. The three tabulated techniques locate the flame in the same zone than the detailed mechanism mainly because the position is imposed by the flow (cfr. the mixture fraction Y_z and the progress variable Y_c in Fig. 4a.). The a posteriori production rates $\dot{\omega}_{Y_c}$ (Fig. 4b.) are different than the a priori estimation (Fig. 3), but the behavior of the three tabulated methods are qualitatively the same. Discrepancies are evident when looking at the intermediate species profiles, such as CO (Fig. 4c.). Globally, only the 2PTF method is also able to predict the concentrations of intermediates, whereas both the PFT and the DFT formalisms are not adequate to describe the chemical structure of gaseous partially-premixed flames [20]. Therefore a multi-regime flamelet method such as 2PTF is expected to better predict the complex structure of spray flames compared to a tabulation method based on a single burning regime such as PFT or DFT. The performances of the tabulated techniques are evaluated in the following for spray flames using the a priori analysis which has been shown to be a significant estimation of the method's behavior.

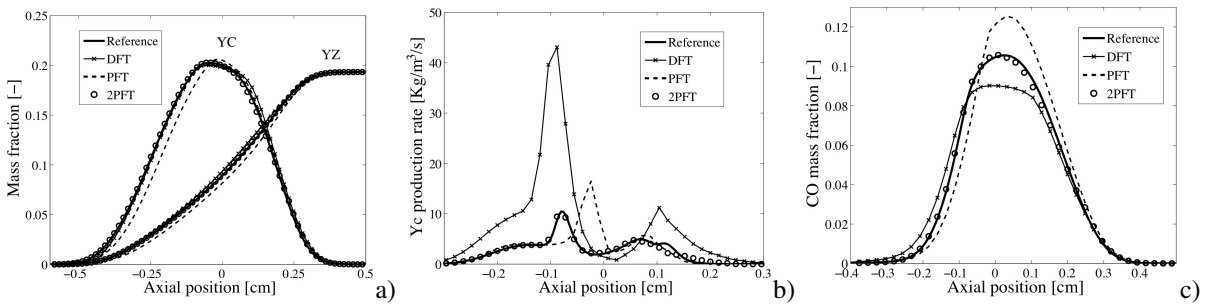

Figure 4. A posteriori a) mixture fraction and progress variable, b) production rate of the progress variable $\dot{\omega}_{Y_c}$ and c) CO profiles for the gaseous flame.

4. Modeling the chemical structure of spray flames

In the following, an axisymmetric mono-disperse counterflow spray flame is considered [21]. Pure fresh air is injected on the left side whereas liquid fuel (spray) and pure air are injected on the right side. The gas and liquid phases at the right injection are characterized by the same temperature $T_g^f = T_l^f$ and axial velocity $v_g^f = v_l^f$, where subscripts g and l denote the gaseous and the liquid phase respectively. The same value of temperature and axial velocity are imposed at both injection sides: $T_g^{ox} = T_g^f$ and $v_g^{ox} = v_g^f$. Through a similarity analysis [22], it could be shown that on the jet axis the mass fraction of the k^{th} species Y_k only depends on the axial coordinate x as well as the density ρ_g, ρ_l, the axial velocity v_g, v_l and the temperature T_g, T_l for both gas and liquid phases. The radial velocities depend also on the radial coordinate r: $u_g = rU_g(x)$ and $u_l = rU_l(x)$.

Governing equations

Assuming a constant pressure gradient in the radial direction $\frac{1}{r}\frac{\partial p}{\partial r} = -J$, the gas phase flow is then described by the following balance equations for mass, radial and axial momentum, energy and species [21]:

$$2\rho_g U_g + \frac{\partial \rho_g v_g}{\partial x} = n_l \dot{m}_l, \tag{10}$$

$$\rho_g U_g^2 + \rho_g v_g \frac{\partial U_g}{\partial x} = \frac{\partial}{\partial x}\left(\mu_g \frac{\partial U_g}{\partial x}\right) + J + n_l \dot{m}_l (U_l - U_g) - n_l \frac{f_r}{r}, \tag{11}$$

$$\begin{aligned}\rho_g v_g c_{p_g} \frac{\partial T_g}{\partial x} = &\frac{\partial}{\partial x}\left(\lambda_g \frac{\partial T_g}{\partial x}\right) - \sum_{k=1}^{K} h_k W_k \dot{\Omega}_k - \left(\sum_{k=1}^{K} \rho_g Y_k V_{kx} c_{p_{gk}}\right)\frac{\partial T_g}{\partial x} \\ &+ n_l \dot{m}_l c_{p_{gF}} (T_l - T_g) - n_l \dot{m}_l q,\end{aligned} \tag{12}$$

$$\rho_g v_g \frac{\partial Y_k}{\partial x} = -\frac{\partial}{\partial x}\left(\rho_g Y_k V_{kx}\right) + W_k \dot{\Omega}_k + \left(\delta_{kF} - Y_k\right) n_l \dot{m}_l, \tag{13}$$

where n_l is the droplet number density, $\dot{m}_l$ is the mass vaporization rate of a single droplet, μ_g is the mixture viscosity, f_i is the i^{th} component of the drag force, $c_{p_{gk}}$ and c_{p_g} are the heat capacity at local constant pressure of species k and of the mixture respectively, q is the heat transferred from the gas to each droplet and δ_{kF} is the Dirac's delta equal to one only for $k = F$ (where subscript F is the index for fuel species), h_k is the molar chemical production rate of the k^{th} species respectively. The system of equations is completed by imposing a constant radial pressure-gradient in the axial direction $\frac{dJ}{dx} = 0$.
The liquid phase flow is obtained solving the following conservation equations [21]:

$$v_l \frac{\partial m_l}{\partial x} = -\dot{m}_l, \tag{14}$$

$$m_l U_l^2 + m_l v_l \frac{\partial U_l}{\partial x} = \frac{f_r}{r}, \tag{15}$$

$$m_l v_l \frac{\partial v_l}{\partial x} = f_x, \tag{16}$$

$$m_l c_{p_l} v_l \frac{\partial T_l}{\partial x} = \dot{m}_l (q - L), \tag{17}$$

$$2 n_l U_l + \frac{\partial n_l v_l}{\partial x} = 0, \tag{18}$$

where $m_l = \frac{4}{3}\pi R_l^3 \rho_q$ is the mass of a single droplet (with R_l the droplet radius and ρ_q the liquid specific mass), L is the latent heat of evaporation and c_{p_l} is the constant pressure heat capacity of the liquid species. The system of equations is completed by assuming a constant radial pressure-gradient in the axial direction $\frac{dJ}{dx} = 0$. The mass vaporization rate of a single droplet $\dot{m}_l$ and the heat transferred from the gas to each droplet q are modeled by the expression for a spherically symmetric single-component droplet obtained from the film temperature model [23, 24].

5. Results on spray flames

The structure of a counterflow spray flame strongly depends on the gaseous flow properties as well as the characteristics of the spray, such as the droplet diameter D_l, the liquid temperature T_l and the liquid volume

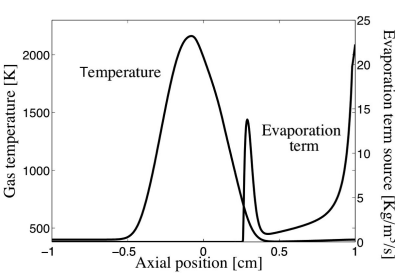

Figure 5. The evaporation source term $n_l \dot{m}_l$ and the gaseous temperature as a function of the axial position in the reference spray flame.

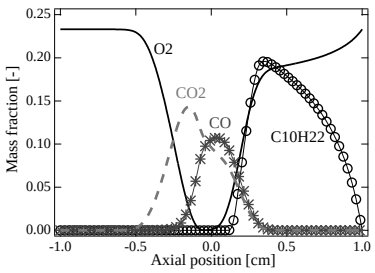

Figure 6. Species profiles as a function of the axial position in the reference spray flame.

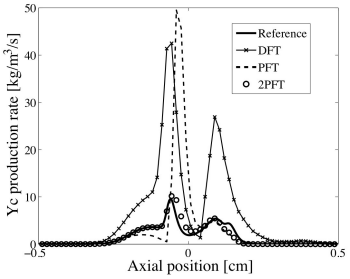

Figure 7. A priori production rate of the progress variable $\dot{\omega}_{Y_c}$ for the reference spray flame.

fraction $\alpha_l = 4/3\pi n_l \left(D_l/2\right)^3$. The capability of the 2PTF tabulation method to capture the structure of a kerosene spray flame is here investigated for different injection conditions. The injection conditions for the reference spray flame are fixed $D_l^f = 40\ \mu m$, $\alpha_l^f = 3.4\ 10^{-3}$, $n_l = 1.0\ 10^{+10}$,$v_g^f = v_l^f = 0.20\ m/s$ and $T_g^f = T_l^f = 400\ K$. The liquid kerosene injected from the right side evaporates due to the evaporation source term $n_l \dot{m}_l$ (Fig. 5). Near the flame front, the gas temperature increases due to the thermal conductivity and, consequently, the source term $n_l \dot{m}_l$ presents a peak ($x \approx 0.4\ cm$). The high temperature region ($-0.4\ cm < x < 0.4\ cm$) is characterized by the presence of intermediate species and products (Fig. 6). The production rate of the progress variable $\dot{\omega}_{Y_c}$ of the reference spray counterflow flame obtained with the detailed scheme is plotted in Fig. 7 in continuous line. At each point, the quantity $\dot{\omega}_{Y_c}$ is now extracted from PFT, DFT and 2PTF look-up tables for the corresponding Y_c, Y_z (and χ^* for the 2PTF method) values to compare in a priori way the three tabulation methods with the reference detailed chemistry spray flame. A first premixed region is found in the zone near the evaporation where a very rich mixture is obtained due to evaporation ($0.1\ cm < x < 0.2\ cm$). As expected from results on gaseous flames, the DFT method overestimates $\dot{\omega}_{Y_c}$ in this zone whereas the PFT method seems to offer more accurate results. A second zone could be observed for $-0.25\ cm < x < -0.1\ cm$ where intermediate species and products are mixed and recombined with the fresh air coming from the left injection. In this region, both the DFT and the PFT method are not adequate to describe this zone. The 2PTF methodology is able to accurately describe the production rate in the whole reaction region characterized by both diffusion and premixed combustion regimes.

5.1 Parametric analysis

The capability of the 2PTF tabulation method to correctly describe the flame structure of a spray flame is evaluated for different boundary conditions.

First of all, the droplet diameter is increased to $D_l^f = 140\ \mu m$ keeping constant the liquid volume fraction at injection by decreasing the density droplet number $n_l = 0.23\ 10^{+9}$. Since the droplets are bigger, evaporation is initially slower and the kerosene remains mainly in liquid phase before reaching the flame front where it evaporates (Fig. 8). Then, the maximum value of gaseous kerosene mass fraction is located in the flame (Fig. 9) and is smaller compared to the reference case ($Y_{C10H22}^{max} \approx 0.12$ for $D_l^f = 140\ \mu m$ and $Y_{C10H22}^{max} \approx 0.21$ for $D_l^f = 40\ \mu m$). The flame presents mainly one partially premixing-like reaction zone (Fig. 10). Neither the PFT method nor the DFT technique are able to reproduce $\dot{\omega}_{Y_c}$. On the contrary, the 2PTF methodology fairly agrees with the reference solution.

The impact of the liquid volume fraction α_l^f on the flame structure and the performances of tabulation methods is also investigated. The liquid volume fraction α_l^f is decreased to $\alpha_l^f = 1.6\ 10^{-3}$ keeping constant the droplet diameter, which means that the overall equivalence ratio is reduced. Evaporation is mainly localized before the flame front (Fig. 11) as confirmed by the position of the maximum value of gaseous kerosene (Fig. 12). The flame presents the two reaction zones identified in the reference case even if the recombination region is characterized by a smaller $\dot{\omega}_{Y_c}$ compared to the reference case (Fig. 13). Once again, the 2PTF method correctly captures the different flame structures.

Finally, the injection velocity is increased to $v_g^f = v_l^f = 1.0\ m/s$ and, as a consequence, the flame strain rate increases too. For this flame, the evaporation zone overlaps a smaller reaction zone (Figs. 14-15). For this flame structure, the three methods mainly capture the production rate $\omega_{\dot{Y}_c}$.

In all studied cases, it has been shown that the 2PTF tabulation method based on gaseous premixed, partially-premixed and diffusion flames is able to correctly describe the different combustion regimes which characterize

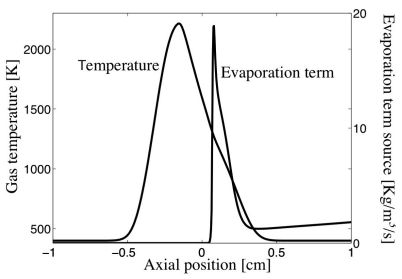

Figure 8. The evaporation source term $n_l \dot{m}_l$ and the gaseous temperature as a function of the axial position of the spray flame with $D_l^f = 140\ \mu m$.

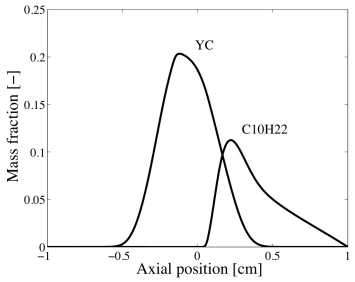

Figure 9. Gaseous kerosene and progress variable profiles as a function of the axial position of the spray flame with $D_l^f = 140\ \mu m$.

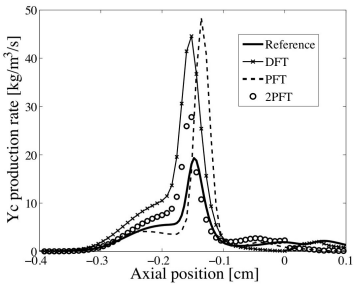

Figure 10. A priori production rate of the progress variable $\dot{\omega}_{Y_c}$ of the spray flame with $D_l^f = 140\ \mu m$.

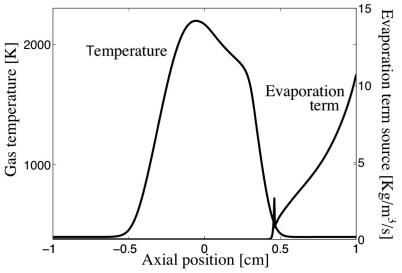

Figure 11. The evaporation source term $n_l \dot{m}_l$ and the gaseous temperature as a function of the axial position of the spray flame with $\alpha_l^f = 1.6\ 10^{-3}$.

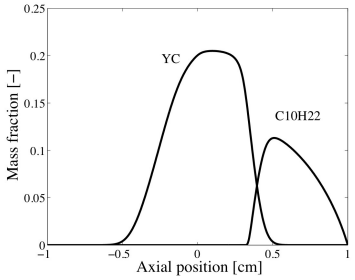

Figure 12. Gaseous kerosene and progress variable profiles as a function of the axial position of the spray flame with $\alpha_l^f = 1.6\ 10^{-3}$.

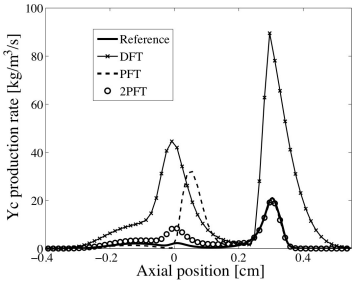

Figure 13. A priori production rate of the progress variable $\dot{\omega}_{Y_c}$ of the spray flame with $\alpha_l^f = 1.6\ 10^{-3}$.

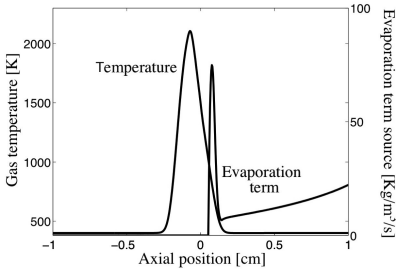

Figure 14. The evaporation source term $n_l \dot{m}_l$ and the gaseous temperature as a function of the axial position for the spray flame with $v_g^f = v_l^f = 1.0\ m/s$.

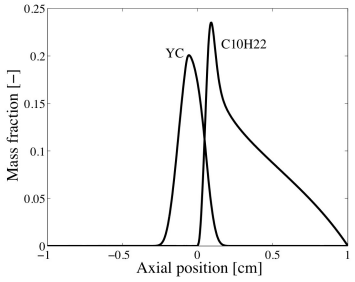

Figure 15. Gaseous kerosene and progress variable profiles as a function of the axial position for the spray flame with $v_g^f = v_l^f = 1.0\ m/s$.

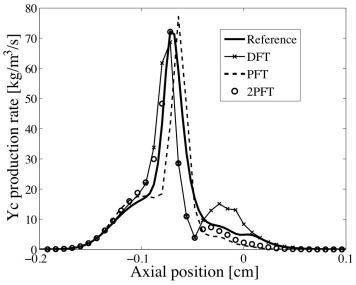

Figure 16. A priori production rate of the progress variable $\dot{\omega}_{Y_c}$ for the spray flame with $v_g^f = v_l^f = 1.0\ m/s$.

the structure of he studied spray flames.

6. Conclusion

To correctly predict spray combustion, a detailed description of the chemical reaction effects is necessary. Tabulation technique is an efficient technique that takes into account detailed chemistry for a reduced computational cost. An evaluation of this approach for spray combustion has been presented in this paper. The new chemical 2PTF table, based on gaseous partially-premixed flames, is parametrized by the progress variable Y_c, describing the progress rate of the reaction, the mixture fraction Y_z, denoting the local equivalence ratio, and the scalar dissipation rate χ^*, which identifies the combustion regime, i.e. $\chi^* = 0$ for premixed flames whereas the maximum values correspond to diffusion flames. Results have been initially compared to those of the classical tabulated chemistry PFT and DFT on gaseous flames using a priori and a posteriori techniques. Then, the tabulated method performances have been investigated a priori on spray flames for different droplet diameter, liquid volume fraction and injection velocity values. In all tested cases, the 2PTF tabulation method better describes the flame structure compared to the classical techniques based on a single archetypal flamelets and it is more adequate for counterflow spray flames.
Nevertheless, the 2PTF method has to be validated on more test cases varying the injection temperature. Moreover, variations of fresh mixture enthalpy are expected to have an important role on spray ßames and their integration in the 2PTF table has to be deeply investigated.

Acknowledgements

The research leading to these results has received funding from the European Community's Seventh Framework Programme (FP7/2007-2013) under Grant Agreement # ACP8-GA-2009-234009. This is part of the 4-year KIAI project started in May 2009, which is a European initiative financed under the FP7 and addresses innovative solutions for the development of new combustors in aero-engines. It aims at providing low NOx methodologies to be applied to design these combustors.

References

[1] X. Jiang, G. A. Siamas, K. Jagus and T. G. Karaylannis. *Progress in Energy and Combustion Science*, 36(2): 131–167, 2010.
[2] E. Gutheil and W. A. Sirignano. *Combustion and Flame*, 113:92–105, 1998.
[3] H. Watanabe, R. Kurose, S. M. Hwang and F. Akamatsu. *Combustion and Flame*, 148:234–248, 2007.
[4] O. Gicquel, N. Darabiha and D. Thévenin. *Proceedings of the Combustion Institute*, 28:1901–1908, 2000.
[5] J. A. van Oijen, F. A. Lammers and L. P.H. de Goey. *Combustion and Flame*, 127:2124–2134, 2001.
[6] N. Peters. *Prog. Energy Comb. Sci.*, 10:(3) 319–339, 1984.
[7] C. Pierce and P. Moin. *Journal of Fluid Mechanics*, 504:73–97, 2004.
[8] E. Knudsen and H. Pitsch. *Combustion and Flame*, 159:242–264, 2012.
[9] J. A. van Oijen and L. P.H. de Goey. *Theory Modeling*, 8:141–163, 2004.
[10] P. D. Nguyen, L. Vervisch, V. Subramanian and P. Domingo. *Combustion and Flame*, 157:43–61, 2010.
[11] W. J.S. Ramaekers, J. A. van Oijen and L. P.H. de Goey. *Flow, Turbulence and Combustion*, 84(3):43–61, 2010.
[12] C. Hollmann and E. Gutheil. *Combust. Sci. and Tech.*, 135:175–192, 1998.
[13] V. Bykov and U. Maas. *Combustion Theory Modeling*, 11(6):839–862, 2007.
[14] Y. Baba and R. Kurose. *J. Fluid. Mech.*, 612:45–79, 2008.
[15] U. Mass and S. B. Pope. *Twenty-Fourth Symposium (International) on Combustion*, 24(1):103–112, 1992.
[16] B. Fiorina, O. Gicquel, L. Vervisch, S. Carpentier and N. Darabiha. *Proceedings of the Combustion Institute*, 30:867–874, 2005.
[17] N. Darabiha. *Combustion Science and Technology*, 86:163–181, 1992.
[18] S. Candel, T. Schmitt, N. Darabiha. *23rd ICDERS*, Irvine, 24-29 July, 2011.
[19] J. Luche. *Elaboration of reduced kinetic models of combustion. Application to a kerosene mechanism.*, Ph.D. thesis, LCSR Orléans, 2003.
[20] B. Fiorina, O. Gicquel, L. Vervisch, S. Carpentier and N. Darabiha. *Combustion and Flame*, 140:147–160, 2005.
[21] N. Darabiha, F. Lacas, J. C. Rolon and S. Candel. *Combustion and Flame*, 95(3):261–275, 1993.
[22] G. Contillo and W. A. Sirignano *Combustion and Flame*, 81:325–340, 1990.
[23] D. B. Spalding. *Fourth Symposium (International) on Combustion*, Pittsburg, 847–864, 1953.
[24] K. K. Kuo. *Principles of Combustion*, John Willey and Sons, 2005.